Evolution of atomicscale surface structures during ion bombardment: A fractal simulation

M. A. Shaheen and D. N. Ruzic

Related Articles

From sponge to dot arrays on (100) Ge by increasing the energy of ion impacts
J. Vac. Sci. Technol. B 30, 06FF12 (2012)

Ion-induced effects on grain boundaries and a-Si:H tissue quality in microcrystalline silicon films
J. Vac. Sci. Technol. A 30, 061512 (2012)

Negative oxygen ion formation in reactive magnetron sputtering processes for transparent conductive oxides
J. Vac. Sci. Technol. A 30, 061306 (2012)

Metal versus rare-gas ion irradiation during Ti1−xAlxN film growth by hybrid high power pulsed magnetron/dc magnetron co-sputtering using synchronized pulsed substrate bias
J. Vac. Sci. Technol. A 30, 061504 (2012)

Proton irradiation energy dependence of dc and rf characteristics on InAlN/GaN high electron mobility transistors [J. Vac. Sci. Technol. B 30, 041206 (2012)]
J. Vac. Sci. Technol. B 30, 043401 (2012)

Additional information on J. Vac. Sci. Technol. A

Journal Homepage: http://avspublications.org/jvsta

Journal Information: http://avspublications.org/jvsta/about/about_the_journal

Top downloads: http://avspublications.org/jvsta/top_20_most_downloaded

Information for Authors: http://avspublications.org/jvsta/authors/information_for_contributors

Evolution of atomic-scale surface structures during ion bombardment: A fractal simulation

M. A. Shaheen and D. N. Ruzic
University of Illinois at Urbana–Champaign, Urbana, Illinois 61801

Surfaces of interest in microelectronics have been shown to exhibit fractal topographies on the atomic scale. A model utilizing self-similar fractals to simulate surface roughness has been added to the ion bombardment code TRIM. The model has successfully predicted experimental sputtering yields of low energy (less then 1000 eV) Ar on Si and D on C using experimentally determined fractal dimensions. Under ion bombardment the fractal surface structures evolve as the atoms in the collision cascade are displaced or sputtered. These atoms have been tracked and the evolution of the surface in steps of one monolayer of flux has been determined. The Ar–Si system has been studied for incidence energies of 100 and 500 eV, and incidence angles of 0°, 30°, and 60°. As expected, normally incident ion bombardment tends to reduce the roughness of the surface, whereas large angle ion bombardment increases the degree of surface roughness. Of particular interest though, the surfaces are still locally self-similar fractals after ion bombardment and a steady state fractal dimension is reached, except at large angles of incidence.

I. INTRODUCTION

Surface roughness is an important factor in the ion–surface interaction phenomenon especially at low incident ion energies (less then 1000 eV) and when the incident ion mass is much less than that of the target atoms' mass. This is because the mean free path of the ions in the solid will be on the order of the surface roughness features.[1]

Surface roughness is a difficult phenomenon to describe mathematically. Often, the degree of surface roughness is described using photographs of surfaces by techniques such as scanning electron microscopy (SEM). A number is then assigned describing the peak value of surface roughness features. This overall characterization may be adequate in certain applications where surface roughness only needs to be described qualitatively. However, for the purposes of modeling of phenomena where surface roughness plays an important role, such as reflection and sputtering at low energies, a more detailed model of surface roughness is needed. In some modeling schemes, surface roughness is described in terms of random distribution of atoms within a certain surface layer.[2] Other models have suggested macroscopic surface features composed of wells and hills.[3] A third approach used the surface binding energy as an adjustable parameter in the simulation[4] to take into account this effect. Adjusting the surface binding energy to account for changes in surface roughness is physically understandable since this binding energy will be a function of the electron cloud at the surface which in turn will depend on the surface features. However, there is no experimental evidence of this effect to guide a proper selection of the binding energy variation.

Surfaces of interest in microelectronics have been shown to exhibit fractal characters. The self-similar fractal dimensions over the length scales of interest to reflection and sputtering have been measured.[5] Some surfaces under bombardment have been shown to be self-affine fractals.[6] A fractal surface repeats a certain generator pattern (or probability distribution) at all scales. If there is only one scale length independent of direction that surface is self-similar. If there is more than one scale length, say two units of directions lying in the plane of the surface to every one unit perpendicular to the plane, it is a self-affine fractal.[7,8]

In this article, and its predecessors[9,10] a fractal surface model is used to simulate effects of surface roughness in the ion bombardment phenomenon. This model has successfully predicted experimental sputtering yields where other models fail as well as better predicting of reflection data especially at higher angles of incidence. This paper extends the work by studying the evolution of surfaces under ion bombardment and calculating the changes in the fractal dimensions. The methodology is then incorporated in the simulation to allow the surface to evolve in steps, and its fractal dimension to change after each step of the bombardment process. Each step is chosen to account for the equivalent flux that would yield one mono-layer coverage: 5000 flights for a 240 Å by 240 Å surface.

In this work, the surfaces generated are self-similar fractals only over some range of scale lengths. Therefore, all mention of fractal dimension refer to a local quantity. Measurements of the self-similar fractal dimension of natural surfaces over particular ranges of scale lengths have been conducted by different groups. Schaefer et al.[11] have studied colloidal aggregates of small silica particles using both x-ray and light scattering. Silica particles with a radius $R_0 \sim 27$ Å were made to aggregate in solution by changes in pH or salt concentration. By the combination of the two different scattering techniques they cover a large range of scales for R_0 up to aggregates with $R \sim 10^4$ Å and they obtained a value for the fractal dimension of 2.12 ± 0.05, over a length scale of 27–10^4 Å. Avnir et al.[12] measured the amount of coverage of a surface by gas adsorption as a
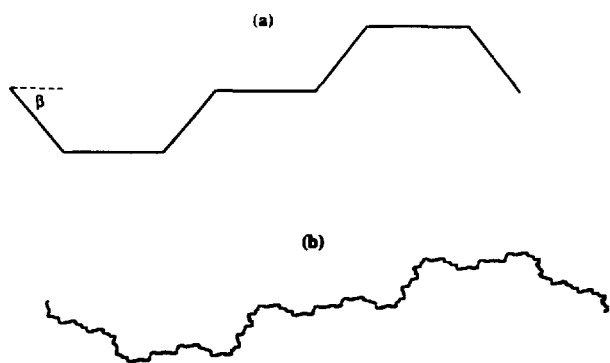
FIG. 1. (a) The volume-preserving generator with fractal dimensions given by $D= \log(7)/\log(3+4\cos\beta)$. For the generator shown, $\beta=59°$ and hence $D=1.20$. (b) The fractal model of dimension 1.10. For a final total width of 240 Å (of the order of ion path length), the length of the fractal segment is about 2 Å (of the order of lattice spacing).

over a range of scales: from the lattice dimension of the target to the average path length of an ion trajectory. This is ensured by making the size of the final fractal generation segment about equal to the lattice dimension of the target material and having enough generations to span a total distance of ~ 100 Å. The choice of the initial generator was made such that it will preserve the volume of the target material and contain some flat segments. This resulted in an odd symmetrical surface $(x,y \rightarrow -x,-y)$ about the flat center of the fractal line. To ensure that the choice of the shape of the initial generator does not affect the simulation results, two generator shapes were used, both having the same fractal dimension and the same property of volume preservation. The results produced differed in both cases only by an amount within the statistical uncertainty.[9]

Previous studies have been aimed at developing a model of a fractal surface that can be used successfully in a computer model to take into account surface roughness effects at low energies without adding adjustable parameters.[9,10] In these studies, the fractal surface model was incorporated into the ion bombardment code TRIM. TRIM is a Monte Carlo simulation that is based on a modified binary collision model. A detailed description of TRIM and its physics is found in Refs. 2 and 15. Several modifications to TRIM were made in order to make use of the surface model. However, the basic physics of the code was preserved. The resulting code FTRIM and its multilayer multicomponent vectorized version VFTRIM[16] were used to study reflection and sputtering by ion bombardment of several ion–target combinations and the results compared to available experimental data. It was found that without altering the parameters of TRIM, or using the surface binding energy as a fitting parameter, the addition of the surface model in VFTRIM leads to better fit to the experimental results at low energies and/or higher angles of incidence angles.[16,17] Figures 2(a) and 2(b) compare some VFTRIM results with Planar TRIM and experimental results for sputtering of deuterium on carbon and argon on silicon, respectively.

As explained above, the fractal dimension is a measurable quantity. It is likely to be a function of the material as well as the method by which the surface was created or altered. In practice, representative samples could be used to measure the resulting fractal dimension of the treated (or grown) samples and that quantity is then used as an input in this code.

To model the evolution of the surface roughness, we define the surface by the uppermost group of atoms in the target with respect to the appropriate scale of the process. In the ion bombardment process, this is determined from the primary knock on atoms (PKA) distribution, which are the first collision partners of the incident ions as it approaches the surface. If enough ions are followed, an accurate description of the surface can be formed. In the beginning of the simulation an initial fractal surface is assumed. This results in a surface–atom distribution that is close to but not identical to the fractal surface assumed. After N cascades have been completely resolved and all atoms involved are either sputtered or displaced in the target, the final positions of the PKAs are determined.

function of the size of the gas atoms, i.e., area versus scale. The log–log plot of their data for Al_2O_3 exhibits the straight line character with a negative slope of 2.79 ± 0.03, which is the surface fractal dimension of the sample. They also report similar measurement[13] for carbon black (2.25 ± 0.09) and Vulcan 3G graphite (2.07 ± 0.01). Mitchell et al.[5] report the measured fractal dimension of sputter deposited gold samples as 2.26 ± 0.04, for fatigued copper 2.34 ± 0.04, and for silicon single crystal 2.07 ± 0.07. Each of these fractal dimensions will be valid over the range where measurement scale is comparable to surface roughness features. These varied from one experiment to another but was generally between tens to thousands of Å. These are also the same scales encountered in the reflection and sputtering phenomenon. The mean free path between collisions is on the order of 4–10 Å and the average path length is typically 100–200 Å.

II. MODELING

In modeling a fractal surface to be used in this simulation, two premises from fractal theory[14] were used to simplify the model: (1) that the intersection of the particle plane of trajectory with a fractal surface of dimension $2.x$ will be a fractal line of dimension $1.x$, and (2) that all such fractal intersection lines will have the same fractal dimension, regardless of the orientation of the intersection plane. With these two facts in mind, a simulation of a fractal surface of dimension $2.x$ was done using a fractal line of dimension $1.x$, including the appropriate manipulation of the orientation of the surface to change the effective orientation of these lines with respect to different particle paths.

Figure 1(a) shows the generator of the intersection of our self-similar fractal surface with the scattering plane of the projectile and scattered atoms. The self-similar fractal dimension D of this generator is set by varying the angle β:
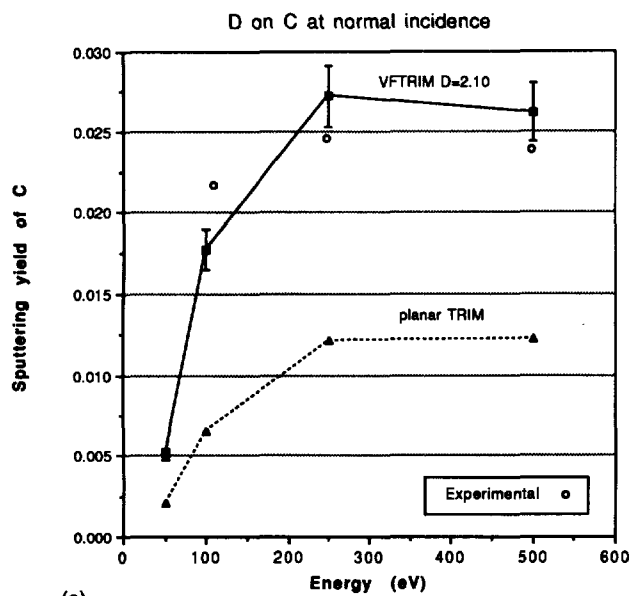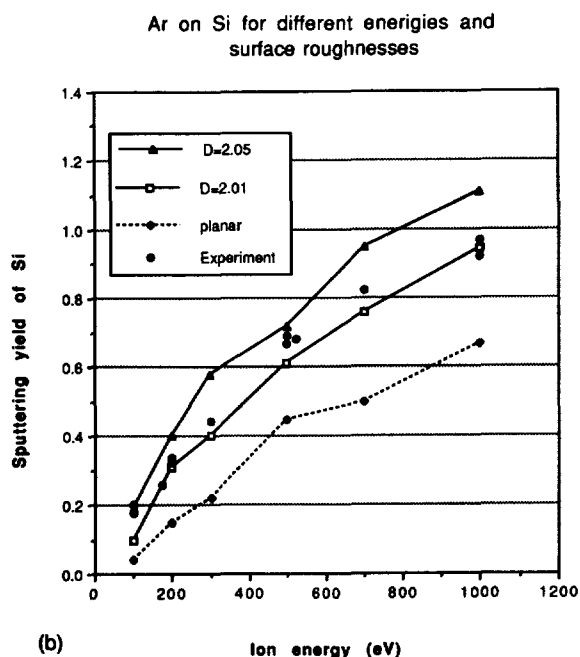
$$D=\frac{\log(7)}{\log(3+4\cos\beta)}.$$

The resulting fractal line, which is shown in Fig. 1(b), is desired to have the same fractal dimension as the generator

D on C at normal incidence

(a)

Ar on Si for different enerigies and surface roughnesses

(b)

δ= 5 Å, D= 1.072

FIG. 3. Generating the intersection plane which simulates the surface from a 2D distribution of PKAs final positions. The smaller the bin size the more detailed the surface would be. Also shown is the scale (bin size) and the fractal dimension of the fractal line.
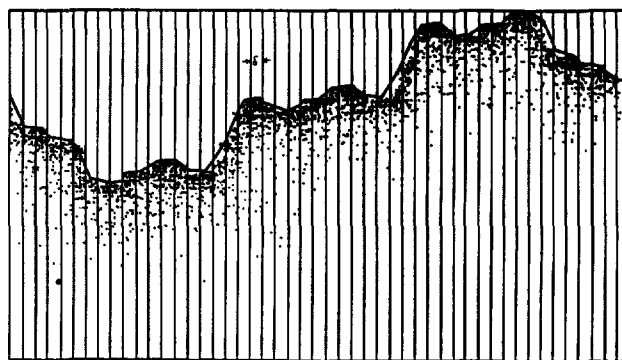
FIG. 2. (a) Sputtering yield of carbon vs energy for deuterium at normal incidence and fractal dimension $D=2.10$. Also shown the planar TRIM and experimental results (Refs. 4 and 21). (b) Sputtering yield of silicon vs energy from VFTRIM for surfaces characterized by fractal dimensions 2.01 and 2.05. Planar TRIM results and experimental results from Ref. 17 are also shown. Both codes used the same surface binding energy of 4.63 eV.

Since these atoms made up the uppermost layer of the surface, their redistribution represents the change in surface features due to this step of ion bombardment. The number of flights N was chosen to be approximately equal to a monolayer surface coverage of bombarding flux. This step of N incident ions in the simulation is referred to as a "generation." For a 240 Å by 240 Å surface, the size of the simulation space, $N=5000$.

The final distribution of surface atoms is then used to generate another surface model for the next generation of the simulation. This is done by a separate algorithm that picks the uppermost atom within a bin of about the size of lattice spacing. This is shown in Fig. 3 where a two-dimensional (2D) distribution of the final positions of the PKAs is used to generate a line representing the surface at a scale or bin size equal to 5 Å. Note that the smaller the bin size, the more detailed the line becomes thus revealing more surface features. This resulting line is used as the intersection line of the surface and planes of trajectories of ions in the following step of the simulation as the surface model input to VFTRIM. Notice that there is nothing beyond the initial fractal surface that forces the atoms to comply to any fractal characteristic.

The simulation is run again, the cascades are resolved, and the final locations of the surface atoms are again determined. This distribution is used to generate the second generation of the surface evolution, and the new surface is used as the input surface model in the simulation for the next step. This process is repeated for many generations and each of these surfaces (actually fractal lines) is studied by a third algorithm to check if they still exhibit fractal characters, as well as calculating the fractal dimension of that particular generation of surface evolution.

The sensitivity of the algorithm to the choice of N is shown in Fig. 4. If N is small there are very few final resting points and the surface appears very rough. If an infinite number of ions were incident on the surface the fractal dimension would match that of the initial generator exactly since any recoil that manages to leave the surface is considered to be sputtered. Eventually every allowable nook and cranny of the original surface would be filled by some PKA, at least down the range of scales of concern here which is about an atom's size.

III. RESULTS

An algorithm FR was used to calculate the fractal dimension at different scales of the initial fractal model and the surface-intersection fractal lines. This was done by di-
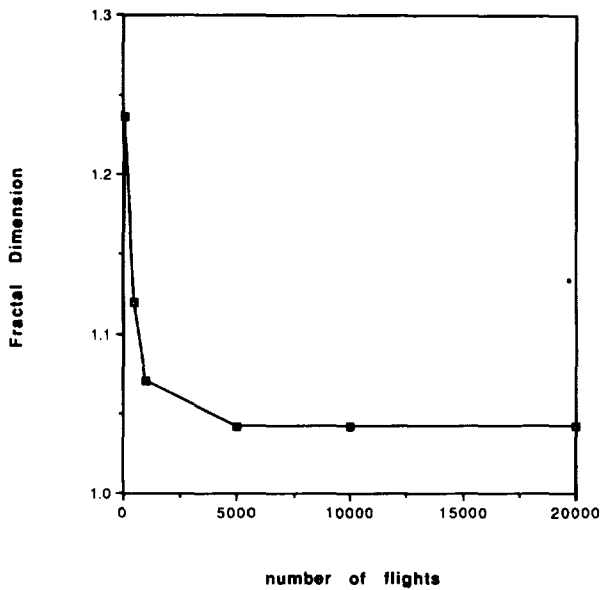
FIG. 4. The variation of the measured fractal dimension with the number of incident ions used to create and follow the surface. At large enough number of flights, the surface features are completely reproduced at the scale of about a lattice spacing and a steady state, in terms of the number of incident ions or length of simulation, is reached.

viding the region into cells of equal size δ, the scale of measurement. Each line is viewed as a finite collection of points, each representing an atom in the intersection plane. The number of cells containing atoms, N, is counted and the fractal dimension is calculated as

$$D = \frac{\log N}{\log N_0},$$

where N_0 is the number of cells in the width of the region. When the scale is large, the cells are large and one cell can contain many points that define the details of the line (roughness features) that are then counted as one surface cell, hence at the largest scale $D=1$. As the scale is decreased the size of the cells decreases and more details of the line are revealed since each cell will contain less surface points. When an initial fractal line of dimension 1.30 was analyzed, the algorithm produced dimensions of 1.314 and 1.304 for $\delta=10$ and 5 Å, respectively.

Figure 5(a) shows the fractal dimension as a function of δ for generators with $D=1.05$, 1.10 and 1.20. The fractal line exhibits the same fractal dimension over a range from the size of the segments in the model (corresponding to the size of the atoms) to the size of the simulation (corresponding to the size of the average path length). Figure 5(b) is a linear plot of the 1–10 Å range. The fractal dimension is almost independent of the scale at the range of 2–50 Å in accordance with the self-similarity property of fractal constructs. The fluctuations are due to the statistical nature of the programming. These figures prove that the used model is indeed fractal (over the specified range of scales). This criterion of independence of the calculated fractal dimension scale is used to determine if an evolved surface still exhibits the fractal character.
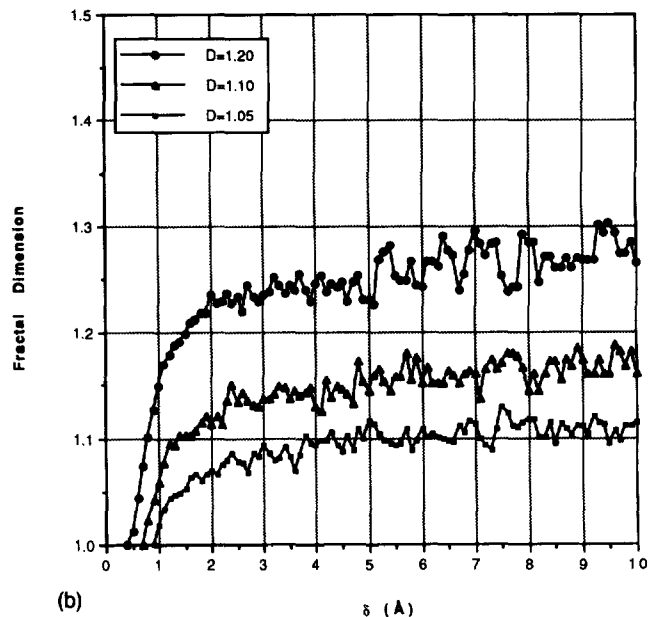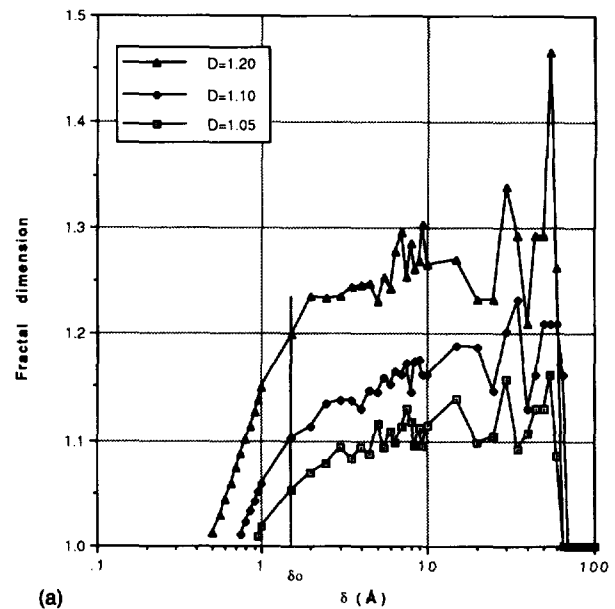

(a)

(b)

FIG. 5. (a) Change in fractal dimension over a wide range of scales for three fractal lines: 1.05, 1.10, and 1.20. The variation is actually smoother than this logarithmic figure shows. (b) Change of the fractal dimension, D, over the range of scale length of the measuring segment. The dimension D remains almost constant over the range of 2–50 Å. δ_0 is the size of the fractal segment.

The different generations of surfaces defined by final PKAs distributions were used as an input to FR and the results for the tenth generation fractal intersection line is shown in Fig. 6. This was produced for the case of 100 eV Ar ions incident on Si at 30° and the initial D for this simulation was 1.05. The fractal dimension, D is fluctuating about 1.07 ± 0.02. The constant fractal dimension over a range of scales is the definition of fractals, therefore it can be concluded that the different generation of surfaces still exhibit the fractal character after ion bombardment.

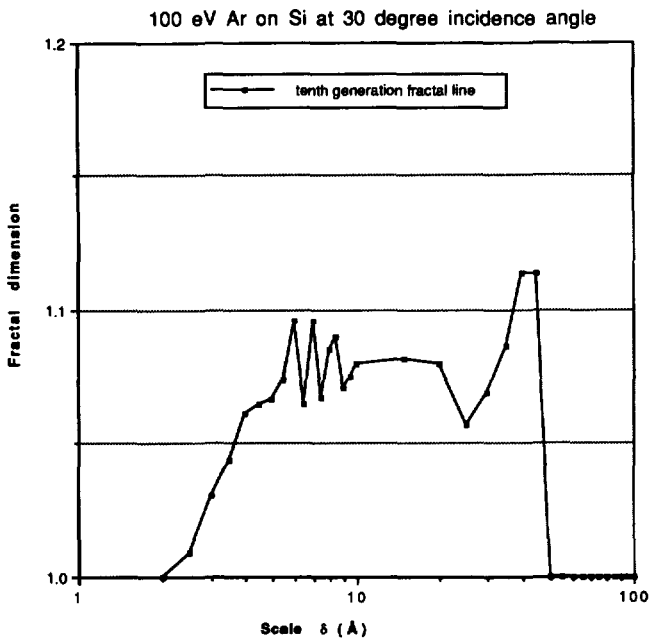Figure 7 shows the variation of the calculated fractal

FIG. 6. Fractal dimension vs scale for the fractal line created by the final positions of the tenth generation of primary knock on atoms. This shows that the surface maintains the fractal character under ion bombardment.
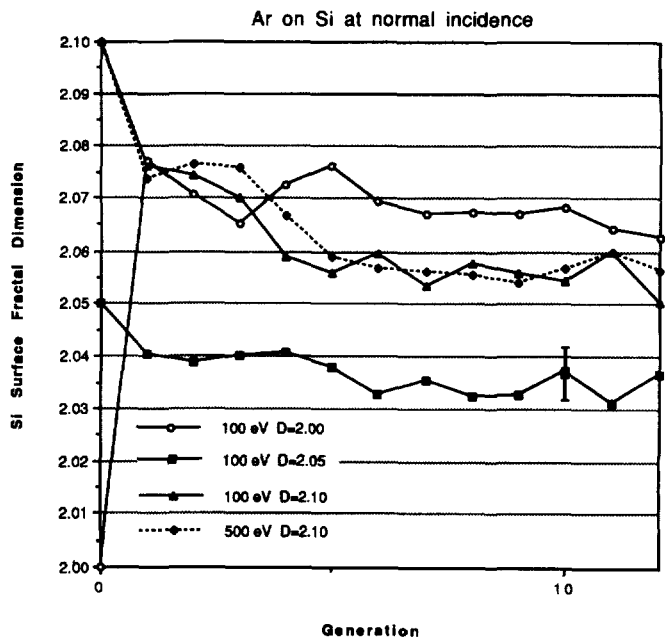

FIG. 7. Change of fractal dimension of the surface of silicon during bombardment by normally incident Ar ions at 100 and 500 eV and for initial fractal dimensions of 2.00, 2.05, and 2.10. This fractal dimension is valid only over the range 2–50 Å. A representative error bar is shown.

dimension for different generations of the surface intersection lines for Ar on Si at normal incidence at energies of 100 and 500 eV and for three initial Si surface fractal dimensions: 2.00, 2.05, and 2.10. The initial model was used to start the simulation and then each evolved surface was used as an input to the following generation. Three features are noticed in Fig. 7. First is that the fractal dimension of the first PKA generation surface rises sharply to about 2.075 for the initially flat surface ($D=2.00$) and drops to about the same value for the initially rough surface ($D=2.10$). For the case when initially $D=2.05$, the variation is smooth. The second feature is that the fractal dimension D decreases slowly to about 2.04–2.06 with ion bombardment for both energies and for all three different initial fractal dimensions. The third feature is that the fractal dimension remains at that level for the subsequent generations. It is thus concluded that steady state fractal dimension is reached and that it is almost independent of the assumed initial fractal dimension.

Though the agreement could be fortuitous, it could be also concluded that this range of fractal dimensions of 2.04–2.06 is characteristic of this Ar on Si system since it is in agreement with an independent measurement of that system [2.07±0.07 (Ref. 5)] and also because it is close to the value that gives the best VFTRIM results fit to experimental data[17] of 2.01–2.05 as shown in Fig. 2(b).

Figure 8 shows the variation of the calculated D with different generations for 100 eV Ar on Si at different incidence angles. Three features are noticed. First, at normal incidence ($\alpha=0°$), D decreases slightly with in bombardment as in Fig. 7 (the larger scale needed underdisplays this feature). Second, at moderately incidence angles ($\alpha=30°$), the surface roughness tends to increase slightly or

remain constant. The third noticeable feature is the large increase in surface roughness with large angle ($\alpha=60°$) ion bombardment. In this last case the fractal character of the surface was largely maintained, but a steady state fractal dimension is not obtained.
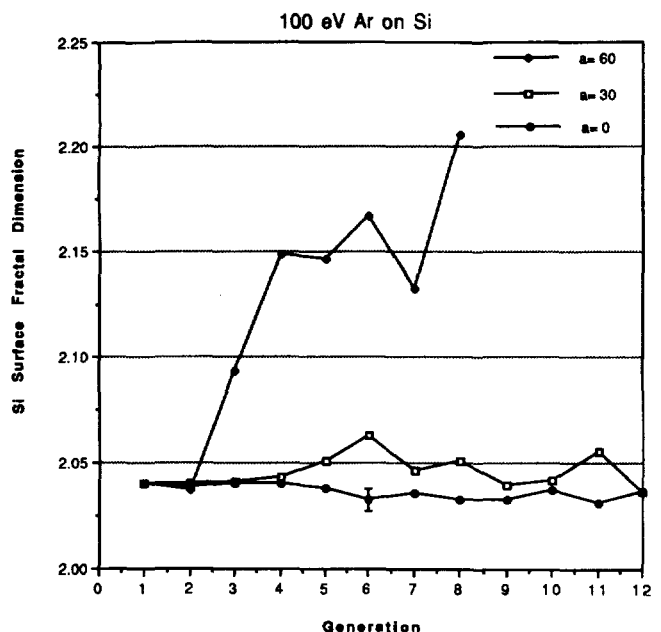

FIG. 8. Change of fractal dimension of a Si surface under bombardment by 100 eV Ar ions at 0°, 30°, and 60° incidence angles. The lower angles lead to a steady state fractal dimension. Higher incidence angles increase D continuously. A representative error bar is shown.

A measure of the statistical dispersion of this simulation was obtained by comparing the resulting D for different initial seed numbers for one typical case, such as that shown in Fig. 7. The maximum error was found to be ± 0.005. This error is due to three statistical processes: (1) the VFTRIM code, (2) the creation of the surface from a distribution of atoms, and (3) measuring D by the box counting method.

IV. DISCUSSION

Although realistic surfaces will still be locally self-similar fractals,[18] they are in general self-affine.[19] The above results were also analyzed in terms of self-affinity using the methods described by Voss[20] and Matsushita.[18] Statistical self-affine dimension (or exponent) H is related to the local fractal dimension D_L through $H = 2 - D_L$, while the global fractal dimension D_G should always be equal to 1, as predicted by the box counting method. Our initial model used a locally self-similar fractal surface from a deterministic generator. Analysis of that generated line for the self-affinity dimension H did not quite produce the expected correspondence for the randomly generated ones, i.e., $H = 2 - D$. The calculated H varied linearly with D, but was about 0.2 less then predicted by this formula for all D as shown in Fig. 9. This could be due to the existance of overhangs in our self-similar models. Self-affine surfaces do not display overhangs. It should also be pointed out that methods of analysis, such as in Ref. 6, that do not detect overhangs will preferably measure self-affine rather than self-similar features. Deterministic self-affine models were also analyzed using the same techniques and they too fell short of the $2 - D$ relation. Our modeling results are still valid locally and show how a locally self-similar surface evolves. A statistical self-affine model would better simulate the overall surface.

The change of surface roughness with ion bombardment is expected since ion bombardment can alter the locations of atoms in the target, especially under long term bombardment as expected in sputtering targets and future fusion devices. The smoothing of the surface due to normal or small angle bombardment can be explained as follows: If the starting surface is rough, this implies that surface atoms are distributed in a peaked fashion, i.e., more atoms at certain locations versus less atoms in others. Small angle ion bombardment tends to displace these atoms in a direction that is generally opposite to the surface peaks. Because of the random nature of this process, the final positions of these atoms will likely be less favorably distributed in peaks or grooves. This means that the resulting surface will be less rough and so the fractal dimension will decrease. In the other case of large angle ion bombardment, the average displacement of the surface atoms will be in a favorable direction that is not the "flat" or horizontal direction. This will lead to an increase in the roughness features in that favored direction.
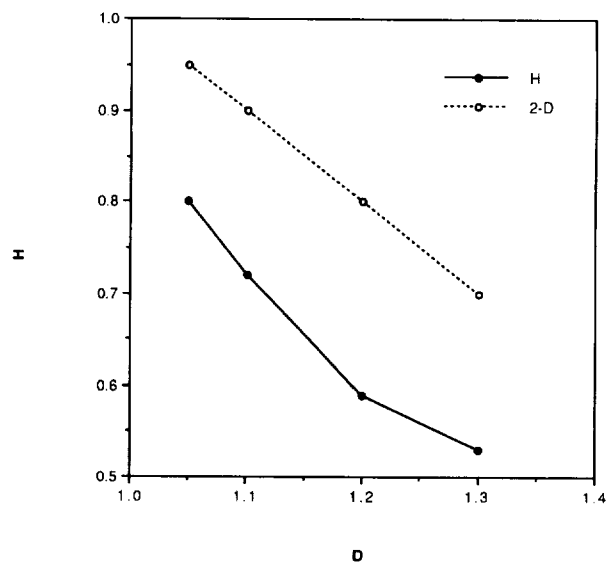
FIG. 9. The self-affinity dimension H vs the (self-similarity) fractal dimension D for the initial fractal models. The expected relation is $H = 2 - D$, but using the approach of Ref. 20, H was found to be about 0.2 less than expected for all D. These surfaces, however, exhibit overhangs, which could explain the difference between the calculated H and the expected one.

ACKNOWLEDGMENTS

[1]*Sputtering by Particle Bombardment*, edited by R. Behrisch (Springer, Berlin, 1981).

[2]J. Biersack and W. Eckstein, Appl. Phys. A **34**, 73 (1984).

[3]A. Pigarov, Y. Igithhanov, Contrib. Plasma Phys. **30**, 71 (1990).

[4]W. Eckstein, A. Sagara, and K. Kamda, J. Nucl. Mater. **150**, 266 (1987).

[5]M. W. Mitchell and D. A. Bonnell, J. Mater. Res. **5**, 2244 (1990).

[6]J. Krim et al., Phys. Rev. Lett. **70**, 57 (1992).

[7]B. Mandelbrot, *The Fractal Geometry of Nature* (Freeman, San Francisco, 1982).

[8]M. Schroeder, *Fractals, Chaos, Power Laws* (Freeman, New York, 1991).

[9]D. Ruzic and H. Chiu, J. Nucl. Mater. **162–163**, 904 (1989).

[10]D. Ruzic, Nucl. Instrum. Methods B **47**, 118 (1990).

[11]D. W. Schaefer et al., Phys. Rev. Lett. **52**, 2371 (1984).

[12]D. Avnir, D. Frain, and P. Pfeifer, Nature **308**, 261 (1984).

[13]D. Avnir, D. Frain, and P. Pfeifer, J. Chem. Phys. **79**, 3566 (1983).

[14]J. Feder, *Fractals* (Plenum, New York, 1988).

[15]J. Biersack and L. Haggmark, Nucl. Instrum. Methods **174**, 252 (1980).

[16]M. A. Shaheen, M. S. dissertation, University of Illinois, 1991.

[17]A. Myers, Ph.D dissertation, University of Illinois, 1991.

[18]M. Matsushita and S. Ouchi, *Dynamics of Fractal Surfaces* edited by F. Family and T. Vicsek (World Scientific, Singapore, 1991).

[19]T. Vicsek, *Fractal Growth Phenomena*, 2nd ed. (World Scientific, Singapore, 1992).

[20]R. Voss, in Ref. 18.

[21]E. Gauthier *et al.*, J. Nucl. Mater. **176-177**, 438 (1990).